Earth and Planetary Science Letters 317-318 (2012) 76–84

Contents lists available at SciVerse ScienceDirect

Earth and Planetary Science Letters

journal homepage: www.elsevier.com/locate/epsl

# Changes in equatorial Pacific thermocline depth in response to Panamanian seaway closure: Insights from a multi-model study

Xiao Zhang [a,*], Matthias Prange [a,b], Silke Steph [b], Martin Butzin [a], Uta Krebs [c], Daniel J. Lunt [d], Kerim H. Nisancioglu [e], Wonsun Park [f], Andreas Schmittner [g], Birgit Schneider [c], Michael Schulz [a,b]

[a] MARUM, Center for Marine Environmental Sciences, University of Bremen, D-28334 Bremen, Germany
[b] Dept. of Geosciences, University of Bremen, D-28334 Bremen, Germany
[c] Institute for Geosciences, Dept. of Geology, Kiel University, D-24118 Kiel, Germany
[d] School of Geographical Sciences, University of Bristol, Bristol BS8 1SS, UK
[e] Bjerknes Centre for Climate Research, Allegaten 55, NO-5007 Bergen, Norway
[f] IFM-GEOMAR, Leibniz-Institut für Meereswissenschaften, D-24105 Kiel, Germany
[g] College of Oceanic and Atmospheric Sciences, Oregon State University, Corvallis, OR 97331, USA

ARTICLE INFO

*Article history:*
Received 4 May 2011
Received in revised form 15 October 2011
Accepted 21 November 2011
Available online xxxx

Editor: P. DeMenocal

*Keywords:*
Pliocene
Panama closure
equatorial Pacific
tropical thermocline
climate modeling

ABSTRACT

The early Pliocene warm phase was characterized by high sea surface temperatures and a deep thermocline in the eastern equatorial Pacific. A new hypothesis suggests that the progressive closure of the Panamanian seaway contributed substantially to the termination of this zonally symmetric state in the equatorial Pacific. According to this hypothesis, intensification of the Atlantic meridional overturning circulation (AMOC) – induced by the closure of the gateway – was the principal cause of equatorial Pacific thermocline shoaling during the Pliocene. In this study, twelve Panama seaway sensitivity experiments from eight ocean/climate models of different complexity are analyzed to examine the effect of an open gateway on AMOC strength and thermocline depth. All models show an eastward Panamanian net throughflow, leading to a reduction in AMOC strength compared to the corresponding closed-Panama case. In those models that do not include a dynamic atmosphere, deepening of the equatorial Pacific thermocline appears to scale almost linearly with the throughflow-induced reduction in AMOC strength. Models with dynamic atmosphere do not follow this simple relation. There are indications that in four out of five models equatorial wind-stress anomalies amplify the tropical Pacific thermocline deepening. In summary, the models provide strong support for the hypothesized relationship between Panama closure and equatorial Pacific thermocline shoaling.


## 1. Introduction

During the warm early Pliocene, ~5.5 to 4 Ma ago, sea surface temperatures in the eastern equatorial Pacific were similar to those of the western tropical Pacific warm pool (Fedorov et al., 2006; Lawrence et al., 2006; Ravelo et al., 2004; Wara et al., 2005). The absence of the eastern equatorial Pacific cold tongue was linked to a weak Walker Circulation, a deep thermocline and low biogenic productivity in the tropical region (Barreiro et al., 2006; Dekens et al., 2007; Fedorov et al., 2006). It has been suggested that this warm equatorial state was responsible for a 3–4 °C warmer-than-present global mean surface temperature and the absence of major ice sheets in the northern hemisphere via processes and teleconnections similar to those that are at work during El Niño states (e.g. Barreiro et al., 2006; Cane and Molnar, 2001; Chiang, 2009; Huybers and Molnar, 2007; Molnar and Cane, 2002; Vizcaíno et al., 2010), although other studies have disputed this (Haywood et al., 2007; Lunt et al., 2008b). Recent studies suggested mechanisms that might have contributed to maintaining the “permanent El Niño-like” climate state, involving a higher frequency of tropical cyclones in the early Pliocene (Fedorov et al., 2010) or a dynamical state approaching “equatorial superrotation” with westerly surface wind anomalies over the equatorial Pacific (Tziperman and Farrell, 2009). However, causes or preconditions for the termination of the equatorial Pacific zonally symmetric state remain obscure. In particular, the original hypothesis by Cane and Molnar (2001), which suggests a key role for the northward displacement and uplift of New Guinea and Halmahera in triggering the climatic switch in the equatorial Pacific, could not be corroborated by climate model experiments thus far (Jochum et al., 2009; Krebs et al., 2011).

A new hypothesis brings the Pliocene closure of the Panamanian seaway into play. Analyzing oxygen isotope and Mg/Ca temperature records from shallow- and deep-dwelling planktonic foraminifers, Steph et al. (2010) reconstructed the Pliocene evolution of the thermocline in the eastern equatorial Pacific and found that gradual shoaling of the thermocline between 4.8 and 4 Ma ago occurred

* Corresponding author.
*E-mail address:* xzhang@marum.de (X. Zhang).

0012-821X/$ – see front matter © 2011 Elsevier B.V. All rights reserved.
doi:10.1016/j.epsl.2011.11.028

synchronously with the progressive closure of the Panamanian seaway and an increase in the Atlantic meridional overturning circulation (AMOC). Based on these findings along with simulation results from the coupled climate model ECBILT-CLIO, Steph et al. (2010) suggested the following chain of events: The early Pliocene shoaling of the Panamanian seaway caused an intensification of the AMOC driven by enhanced North Atlantic Deepwater (NADW) formation. Enhanced NADW production resulted in an increased volume of the “cold water sphere” and hence to upward thermocline shifts in the global ocean transmitted by baroclinic oceanic adjustment processes (Cessi et al., 2004; Clement and Peterson, 2008; Goodman, 2001; Haarsma et al., 2008; Huang et al., 2000; Lopes dos Santos et al., 2010; Timmermann et al., 2005). In the eastern tropical Pacific, the thermocline shoaling preconditioned the equatorial cold tongue state, before intensified trade winds (probably related to high-latitude glaciation) could bring cold waters to the surface after ~3.6 Ma.

In this study, we shall further test the hypothesized relationship between Panama closure, AMOC strength and equatorial Pacific thermocline depth. How robust are the model results presented by Steph et al. (2010) among different models? How strong is the influence of changes in AMOC strength on tropical Pacific thermocline depth? How may wind-stress feedbacks affect the Pacific thermocline? To address these questions, we analyze and compare climate model results from twelve different Panamanian seaway-closure simulations.

## 2. Model simulations and analysis

A total of twelve experiments with eight different models are analyzed in this study. In contrast to coordinated model intercomparison projects, the model experiments were set up independently, such that differences in boundary conditions, Panama seaway depth, etc. exist. Table 1 provides an overview of the different models and setups. Five models include a dynamic atmosphere, thus allowing for, e.g., wind-stress feedbacks (HadCM3, CCSM2, CCSM3, KCM and ECBILT-CLIO). The other three models (UVIC, BREMIC/LSG, MIT) apply prescribed modern wind fields to force the ocean. All models use present-day or pre-industrial boundary conditions, except for the HadCM3 experiment in which mid-Pliocene boundary conditions are applied. The mid-Pliocene boundary conditions include reduced ice-sheet sizes, Pliocene vegetation distribution and enhanced atmospheric $CO_2$ concentration (400 ppmv). As a result, the global mean surface temperature is ca. 3 °C warmer compared to pre-industrial conditions (Lunt et al., 2008a).

Applying different seaway depths and ocean vertical diffusivities, Schneider and Schmittner (2006) performed a series of sensitivity experiments with the UVIC model. These experiments are referred to as UVIC3sh, UVIC3in, UVIC6sh and UVIC6in, where “3”, “6”, “sh” and “in” stand for low vertical diffusivity (0.3 $cm^2\,s^{-1}$ in the upper ocean), high vertical diffusivity (0.6 $cm^2\,s^{-1}$ in the upper ocean), shallow seaway (130 m) and intermediate-depth seaway (700 m). This allows us to examine the effects of both vertical mixing and Panamanian sill depth on the behavior of the Pacific equatorial thermocline in one and the same model. We note that the UVIC simulations with a 2000 m deep Panamanian gateway performed by Schneider and Schmittner (2006) were not included in this paper, as the results of these simulations are nearly identical to the UVIC runs with a 700 m deep seaway.

Four previously unpublished Panama experiments have been conducted and are included in this study. ECBILT-CLIO was used in the first new experiment. Apart from a shallower Panamanian sill depth (415 m), the experimental design is identical to that described by Prange and Schulz (2004) who applied a 700 m deep seaway in their original study. In the second previously unpublished experiment, we employed the global ocean model BREMIC/LSG coupled to a simplified energy balance model. The closed-Panama control run with modern boundary conditions is described in Butzin et al. (2005, 2011). In the corresponding open-Panama experiment, the model has been integrated into a new equilibrium after implementing a 500 m deep seaway by replacing three land grid cells by ocean cells. The third new experiment employed the comprehensive Community Climate System Model version 3 (CCSM3) in its low-resolution version (Collins et al., 2006; Yeager et al., 2006). The

**Table 1**
Overview of the model simulations analyzed in this paper. “AMOC” refers to the North Atlantic overturning streamfunction maximum. Four different experiments were performed with the UVIC model which differs in Panamanian seaway depth and vertical mixing. These experiments are denoted by “3”, “6”, “sh” and “in” which stands for low vertical diffusivity (0.3 $cm^2\,s^{-1}$ in the upper ocean), high vertical diffusivity (0.6 $cm^2\,s^{-1}$ in the upper ocean), shallow seaway (130 m) and intermediate depth seaway (700 m). With ECBILT-CLIO, two experiments with different seaway depths were carried out, denoted by EC415 and EC700, which stands for 415 m and 700 m depth, respectively.

| Model name | Atmosphere component | AMOC (Sv); closed/open seaway | Seaway depth (m) | Net eastward flow through seaway (Sv) | Remark | Reference for model | Reference for open-Panama experiment |
|---|---|---|---|---|---|---|---|
| UVIC 3sh | Energy-moisture balance model | 13/11 | 130 | 5 | Vert. diffusivity: 0.3–1.3 $cm^2\,s^{-1}$ | Weaver et al. (2001) | Schneider and Schmittner (2006) |
| UVIC 3in | Energy-moisture balance model | 13/5 | 700 | 10 | Vert. diffusivity: 0.3–1.3 $cm^2\,s^{-1}$ | Weaver et al. (2001) | Schneider and Schmittner (2006) |
| UVIC 6sh | Energy-moisture balance model | 18/17 | 130 | 7 | Vert. diffusivity: 0.6–1.6 $cm^2\,s^{-1}$ | Weaver et al. (2001) | Schneider and Schmittner (2006) |
| UVIC 6in | Energy-moisture balance model | 18/13 | 700 | 16 | Vert. diffusivity: 0.6–1.6 $cm^2\,s^{-1}$ | Weaver et al. (2001) | Schneider and Schmittner (2006) |
| BREMIC/LSG | Simplified energy balance model | 18/10 | 500 | 14 | | Maier-Reimer et al. (1993), Prange et al. (2003) | This study |
| MIT (OGCM) | Mixed boundary conditions | 31/28 | 1000 | 16 | No Arctic Ocean | Marshall et al. (1997) | Nisancioglu et al. (2003) |
| HadCM3 | General circulation model | 20/10 | 370 | 8 | Mid-Pliocene boundary conditions | Gordon et al. (2000) | Lunt et al. (2008a) |
| CCSM2 | General circulation model | 14/12 | 800 | 12 | | Kiehl and Gent (2004), Prange (2008) | Steph et al. (2006a) |
| CCSM3 | General circulation model | 16/8 | 1475 | 11 | | Collins et al. (2006), Yeager et al., (2006) | This study |
| KCM | General circulation model | 14/11 | 1200 | 13 | | Park et al. (2009) | This study |
| EC415 (ECBILT-CLIO) | Quasi-geostrophic circulation model | 27/19 | 415 | 11 | | Goosse and Fichefet (1999), Opsteegh et al. (1998) | This study |
| EC700 (ECBILT-CLIO) | Quasi-geostrophic circulation model | 27/15 | 700 | 14 | | Goosse and Fichefet (1999), Opsteegh et al. (1998) | Prange and Schulz (2004) |

resolution of the atmospheric component is T31 (~3.75° transform grid) with 26 levels, while the ocean component has a nominal resolution of 3° with 25 levels in the vertical (higher meridional resolution of 0.9° around the equator). Along with a 1000-year-integrated control run with present-day boundary conditions, we performed another 1000-year integration with a 1500 m deep Panamanian seaway by replacing three land grid cells by ocean grid cells between North and South America. Both runs were initialized with present-day observational data. The Kiel Climate Model, KCM (Park et al., 2009), was used in the fourth previously unpublished experiment. In the simulations described here, the atmospheric resolution is T31 with 19 levels. The horizontal ocean resolution is based on a 2° Mercator mesh and is on average 1.3°, with enhanced meridional resolution of 0.5° close to the equator, and with 31 levels in the vertical. In the open-Panama run, the seaway is 1200 m deep and four grid cells wide. Control and sensitivity runs were integrated for 1000 years.

All results presented in this study refer to long-term annually averaged quantities from equilibrated model runs. In order to analyze the effect of an open Panamanian seaway on the Pacific equatorial thermocline in a specific model, we calculated the depth of the 20 °C isotherm (referred to as Z20) in the experiment with open gateway and compare it to the corresponding model run with closed gateway. We note that the thermocline is generally defined as the depth at which the vertical temperature gradient is at maximum. In numerical (z-coordinate) ocean models, however, the search for this maximum would always result in thermocline depths that correspond exactly to depths of grid points. Hence changes, which are smaller than the vertical grid spacing would not be observed when using the maximum temperature gradient for thermocline depth calculations. By contrast, the depth of an isotherm is not bound to the grid spacing; an isotherm can well reside between two grid points in the vertical and its depth can be found by linear interpolation of the gridded temperature field. Z20 is a commonly used quantity to specify the depth of the Pacific equatorial thermocline, since it closely matches the depth of the maximum vertical temperature gradient under modern climate conditions in that region (e.g. Fedorov and Philander, 2001; Harrison and Vecchi, 2001; McPhaden and Yu, 1999; Steph et al., 2010; Timmermann et al., 2007). It should be noted that even though the HadCM3 experiment has a higher global mean temperature due to Pliocene boundary conditions, Z20 still matches the depth of the maximum vertical temperature gradient in the equatorial Pacific.

## 3. Results and discussion

All models simulate an eastward net volume transport through the Panamanian gateway (i.e. from the Pacific to the Atlantic). The flow of relatively low-saline Pacific water into the Atlantic results in a freshening of the surface North Atlantic in all the models (Fig. 1) which, in turn, leads to weakening of NADW formation and hence reduction of the AMOC.

Fig. 2 displays the effect of an open Panama gateway on the depth of the Pacific tropical thermocline (Z20). The models show a general deepening of the equatorial thermocline when the seaway is open, except for the shallow-gateway UVIC runs and the MIT model. This implies that 9 out of 12 model experiments – and in particular all experiments with a coupled dynamic atmosphere model – support the relationship between Panama closure and the tropical Pacific thermocline hypothesized by Steph et al. (2010).

Z20 changes (i.e. differences between model runs with open Panama gateway minus corresponding model runs with closed isthmus) averaged over the Niño-3 region (150°W–90°W, 5°N–5°S) are plotted against AMOC changes in Fig. 3. We first consider only those models that do not include wind-stress feedbacks. The graph shows that models, which exhibit equatorial thermocline shoaling in response to an open Panamanian seaway (UVIC3sh, UVIC6sh, MIT), simulate only minor changes in the AMOC. In these models, the removal of Pacific thermocline water by the upper-ocean outflow from the Pacific to the Atlantic leads to Pacific thermocline shoaling (cf. Fig. 6 in Sarnthein et al., 2009). In models that simulate larger AMOC changes, Z20 increases in response to an open seaway (UVIC3in, UVIC6in, BREMIC/LSG). In these cases, the effect of a weakened AMOC overcompensates the effect of Pacific thermocline water removal through the gateway, i.e. reduced formation of deepwater in the northern North Atlantic leads to a decrease in the volume of the “cold-water sphere” and, hence, to downward thermocline-shifts in the global ocean (Cessi et al., 2004; Clement and Peterson, 2008; Goodman, 2001; Haarsma et al., 2008; Huang et al., 2000; Lopes dos Santos et al., 2010; Timmermann et al., 2005). An AMOC change of at least ~4 Sv ($1\ Sv = 10^6\ m^3/s$) is required for this overcompensation (Fig. 3). We find that the change in Z20 scales almost linearly with the change in AMOC as indicated by the regression line in Fig. 3, i.e. the greater the reduction in AMOC strength, the stronger the deepening of the Pacific equatorial thermocline. This result supports the notion by Steph et al. (2010) that the Pliocene shoaling of the equatorial Pacific thermocline was the result of a global oceanic adjustment in response to AMOC strengthening, which, in turn, was induced by the gradual closing of the Panamanian seaway.

The models with dynamic atmosphere (CCSM2, CCSM3, HadCM3, KCM and ECBILT-CLIO), however, do not fit to this linear regression. In CCSM2, CCSM3, HadCM3 and KCM, the Z20 differences lie above the regression line calculated from the models without wind-stress feedback, whereas the Z20 response in ECBILT-CLIO is relatively small given the large AMOC change (Fig. 3). We note that basically the same picture emerges when plotting Z20 changes against percentage AMOC changes instead of absolute AMOC changes (not shown). These findings suggest a substantial modification of the AMOC-Z20 relationship through dynamical processes in the atmosphere and air–sea coupling.

In order to further elucidate these processes, we plotted changes in equatorial zonal wind stress along with changes in Z20 for CCSM2, CCSM3, HadCM3, KCM and ECBILT-CLIO (EC415 and EC700) in Fig. 4. In all these models with a dynamic atmosphere, weakening of the AMOC induced by an open Panamanian seaway causes an anomalous northern-to-southern hemisphere sea-surface temperature gradient (the so-called “seesaw effect”, e.g. Stocker (1998)) (Fig. 5) which, in turn, induces a southward shift of the Intertropical Convergence Zone (cf. Lunt et al., 2008a; Steph et al., 2006a; Steph et al., 2010) and associated wind anomalies over the equatorial Pacific that are mostly northeasterly (Broccoli et al., 2006) (Fig. 6). Note that in Fig. 5 some models show a local sea-surface temperature warming in the Nordic Seas despite a general cooling of the northern hemisphere (in particular CCSM2 and HadCM3), which is attributable to a reduced “Arctic Throughflow” from the North Pacific to the North Atlantic (via Bering Strait) when the Panamanian gateway is open (Sarnthein et al., 2009).

On timescales longer than that of equatorial adjustment, generally stronger easterlies result in an increase in the mean depth of the equatorial Pacific thermocline (Vecchi and Soden, 2007; Vecchi et al., 2006). We propose that this wind-stress effect is likely to be responsible for the relatively large central Pacific thermocline responses in CCSM2, HadCM3 and KCM (Fig. 3). Only in the easternmost region of the equatorial Pacific, the stronger easterlies tend to shoal the thermocline in these models. In CCSM3, a westerly wind-stress anomaly west of 135°W tends to move surface water into the Niño-3 region, leading to a substantial deepening of the thermocline in that area (Fig. 4). In ECBILT-CLIO, the largest easterly wind-stress anomalies are found west of 150°W (Figs. 4 and 6). Such easterly wind-stress anomalies over the western Pacific tend to shoal the equatorial thermocline in the central and eastern Pacific (Timmermann et al., 2007). Consequently, the wind-stress response weakens rather than amplifies changes in the depth of the equatorial thermocline in ECBILT-

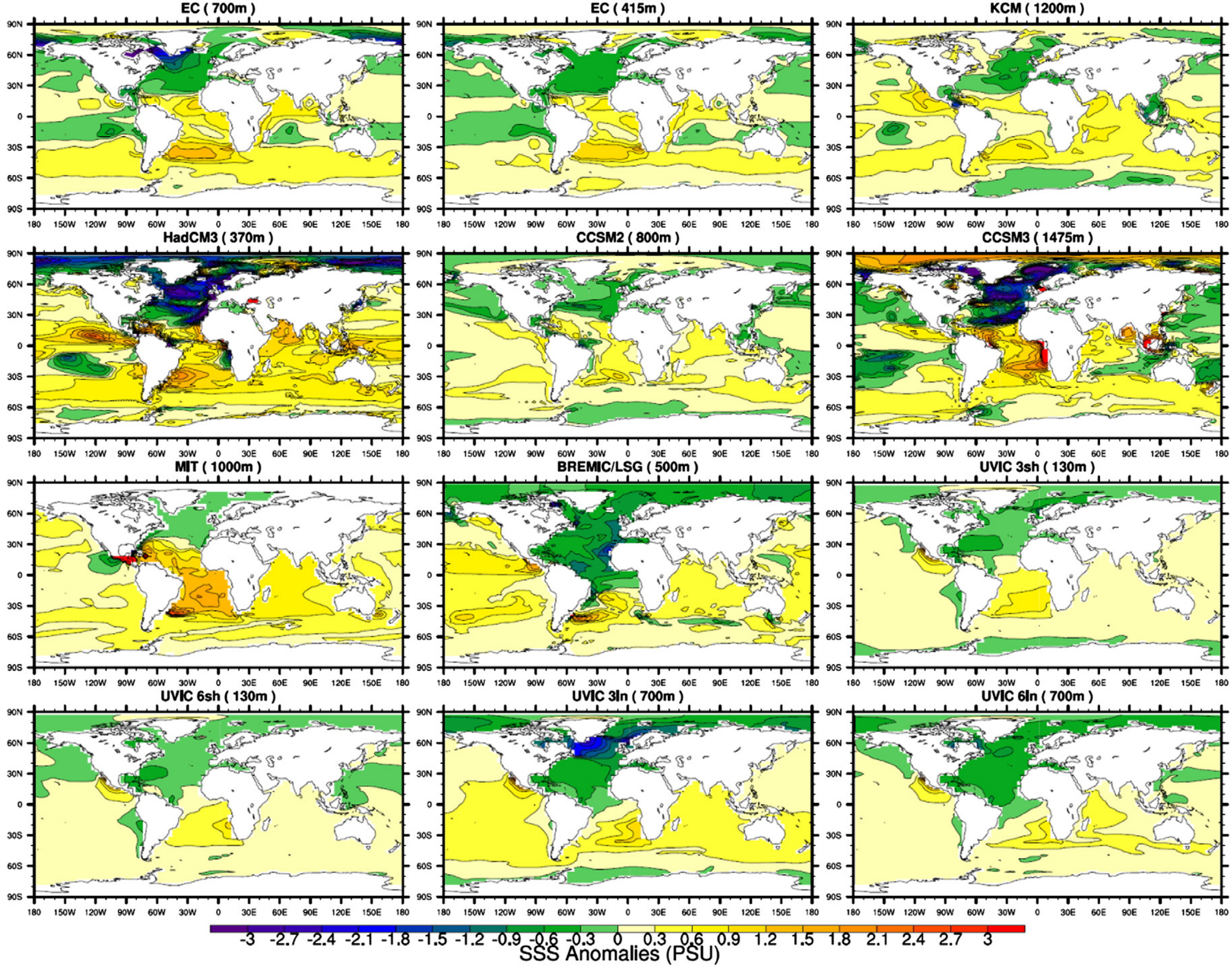


**Fig. 1.** Effect of an open Panamanian seaway on global sea surface salinity (SSS): Difference in SSS (psu) between runs with open and closed Panama gateway (i.e. open minus closed) in the various models. The depth of the seaway in the different experiments is given in parentheses.

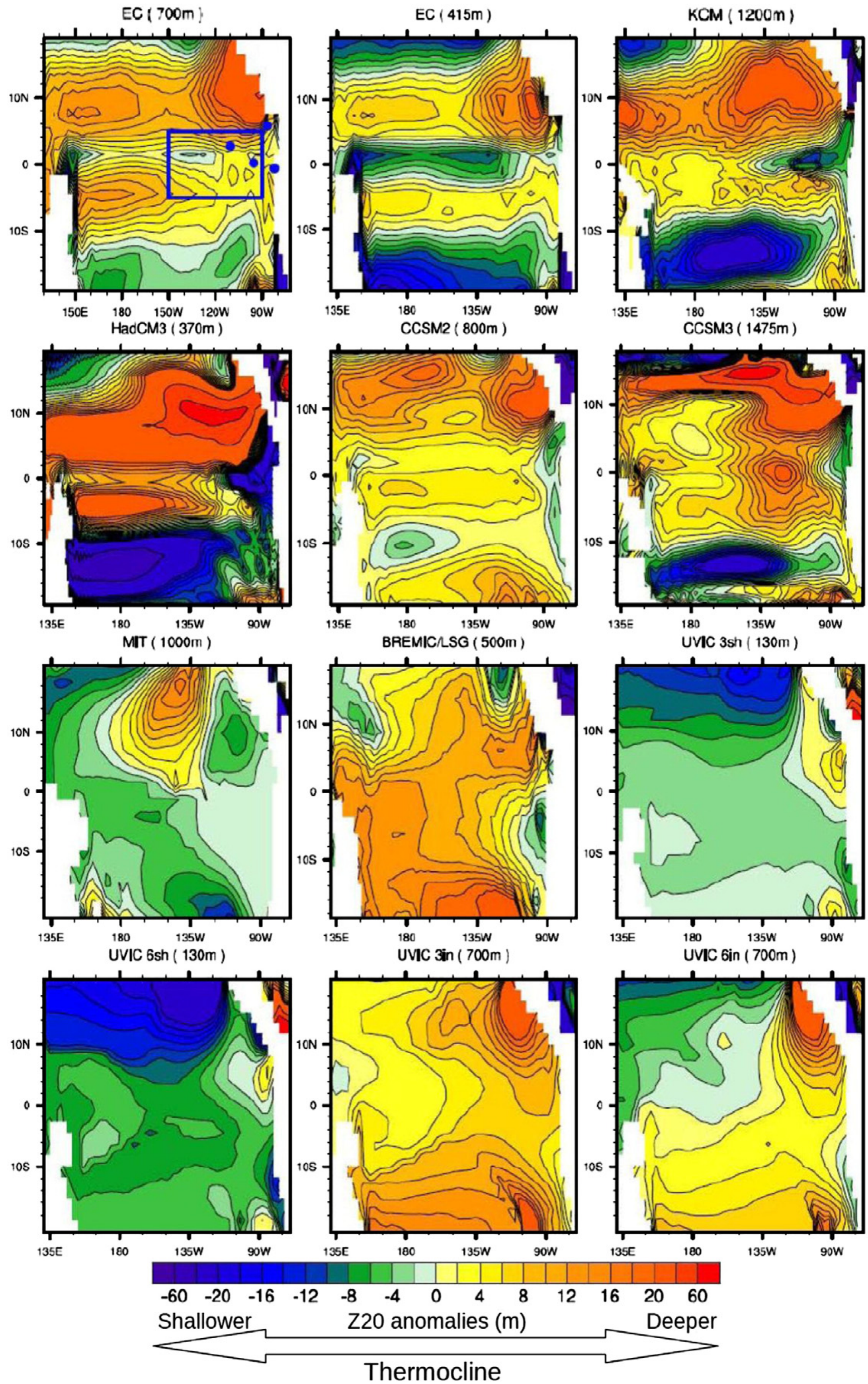


**Fig. 2.** Effect of an open Panamanian seaway on the equatorial Pacific thermocline: Difference in the depth of the 20 °C isotherm (Z20) between runs with open and closed Panama gateway (i.e. open minus closed) in the various models. The blue box marks the Niño-3 region. The blue dots indicate the locations of sediment cores from which Pliocene tropical thermocline shoaling has been inferred (Cannariato and Ravelo, 1997; Steph et al., 2006b; Steph et al., 2010; Wara et al., 2005). The depth of the seaway in the different experiments is given in parentheses. (For interpretation of the references to color in this figure legend, the reader is referred to the web version of this article.)

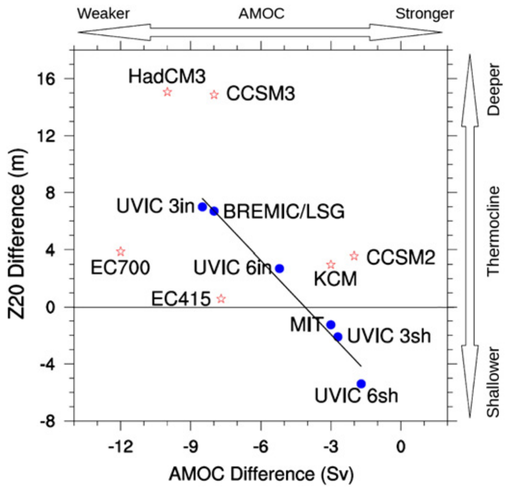


**Fig. 3.** Effect of an open Panamanian seaway on the eastern equatorial Pacific thermocline and AMOC strength. "Z20 difference" refers to the difference in the depth of the 20 °C isotherm in the Niño-3 region (i.e. averaged over the region 150°W–90°W, 5°N–5°S) between runs with open and closed Panama gateway (i.e. open minus closed), while "AMOC difference" refers to the change in the North Atlantic overturning streamfunction maximum (open minus closed) in the various models. The dots mark models without wind-stress feedback, whereas models that include a dynamic atmosphere are marked by stars. The regression line has been calculated by only taking the models without wind-stress feedback into account.

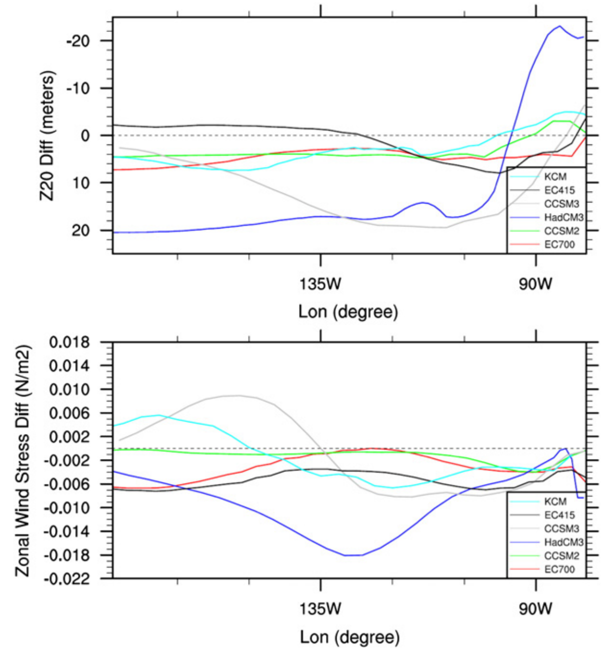


**Fig. 4.** Effect of an open Panamanian seaway on equatorial Pacific thermocline depth and zonal wind-stress (both averaged over 5°N–5°S) in models that include a dynamic atmosphere. "Z20 diff" refers to the difference in the depth of the 20 °C isotherm between runs with open and closed Panama gateway (i.e. open minus closed), while "Zonal Wind Stress Diff" refers to the change in equatorial Pacific zonal wind-stress (open minus closed) in the various models.

CLIO. However, ECBILT-CLIO has to be considered less reliable in simulating tropical atmosphere dynamics than the comprehensive models CCSM2, CCSM3, HadCM3, and KCM due to simplified governing equations (quasi-geostrophic approximation) and a low resolution (~5.6° with only 3 levels in the vertical).

In summary, all experiments with comprehensive coupled climate models suggest that wind-stress effects amplify the thermocline deepening induced by AMOC slowing. However, besides tropical air–sea momentum fluxes, tropical and extra-tropical surface heat and freshwater fluxes cannot be ruled out as drivers for equatorial thermocline changes. It is further worth noting that even those models that simulate an equatorial Pacific thermocline deepening in the Niño-3 region in response to an open Panama gateway, do not necessarily capture the thermocline deepening at the sites of the sediment cores from which Steph et al. (2010) inferred their hypothesis (Fig. 2). This mismatch can most likely be attributed to the rather coarse grid resolutions in all the models, which were designed for large-scale climate simulations and are hardly capable of simulating regional winds and ocean currents in the tropical eastern Pacific region.

The UVIC sensitivity experiments (Schneider and Schmittner, 2006) reveal the important effect of vertical diffusivity on the Panamanian throughflow, the sensitivity of the AMOC, and the equatorial Pacific thermocline. In both the shallow-gateway experiments (UVIC3sh, UVIC6sh) and the intermediate-depth runs (UVIC3in, UVIC6in), stronger vertical mixing leads to a stronger eastward throughflow (Table 1). This finding is consistent with the reasoning of Nof and Van Gorder (2003) who showed that eastward flow through the Panamanian gateway depends on diapycnal mixing and/or NADW formation, with NADW formation in turn being dependent on diapycnal mixing (e.g. Schneider and Schmittner, 2006). The UVIC runs further show that the gateway-induced AMOC changes are stronger in the low-diffusivity runs than in the high-diffusivity experiments (despite smaller Panamanian throughflow). This finding is consistent with earlier studies that suggested enhanced stability of the AMOC to North Atlantic surface salinity perturbations with increasing vertical mixing (Nof et al., 2007; Prange et al., 2003; Schmittner and Weaver, 2001). As a result, the UVIC low-diffusivity experiments (UVIC3sh, UVIC3in) exhibit a larger Z20 response than the corresponding high-diffusivity cases (UVIC6sh, UVIC6in).

## 4. Summary and conclusions

The major findings of our multi-model study can be summarized as follows:

(1) All model experiments with an open Panama gateway show an eastward Panamanian net throughflow, leading to a reduction in NADW formation and hence AMOC strength compared to the corresponding closed-Panama case.
(2) In the absence of wind-stress feedbacks, deepening of the equatorial Pacific thermocline induced by an open Panamanian seaway scales almost linearly with the throughflow-induced reduction in AMOC strength, i.e. a weaker (stronger) AMOC is associated with a deeper (shallower) equatorial Pacific thermocline.
(3) All models with a dynamic atmosphere simulate a deepening of the equatorial Pacific thermocline in response to an open Panama gateway, whereas models without dynamic atmosphere require a minimum reduction of the AMOC (ca. 4 Sv) to simulate the thermocline deepening.
(4) The results from the comprehensive coupled climate models suggest that wind-stress effects amplify the deepening of the equatorial Pacific thermocline in response to throughflow-induced AMOC slowing.
(5) The simulated volume flux of the Panamanian throughflow and the gateway's impact on the AMOC and the depth of the equatorial Pacific thermocline depend sensitively on the parameterization of poorly constrained parameters like ocean vertical diffusivity.

**Fig. 5.** Effect of an open Panamanian seaway on global sea surface temperature (SST): Difference in SST (K) between runs with open and closed Panama gateway (i.e. open minus closed) in the various models. The depth of the seaway in the different experiments is given in parentheses.

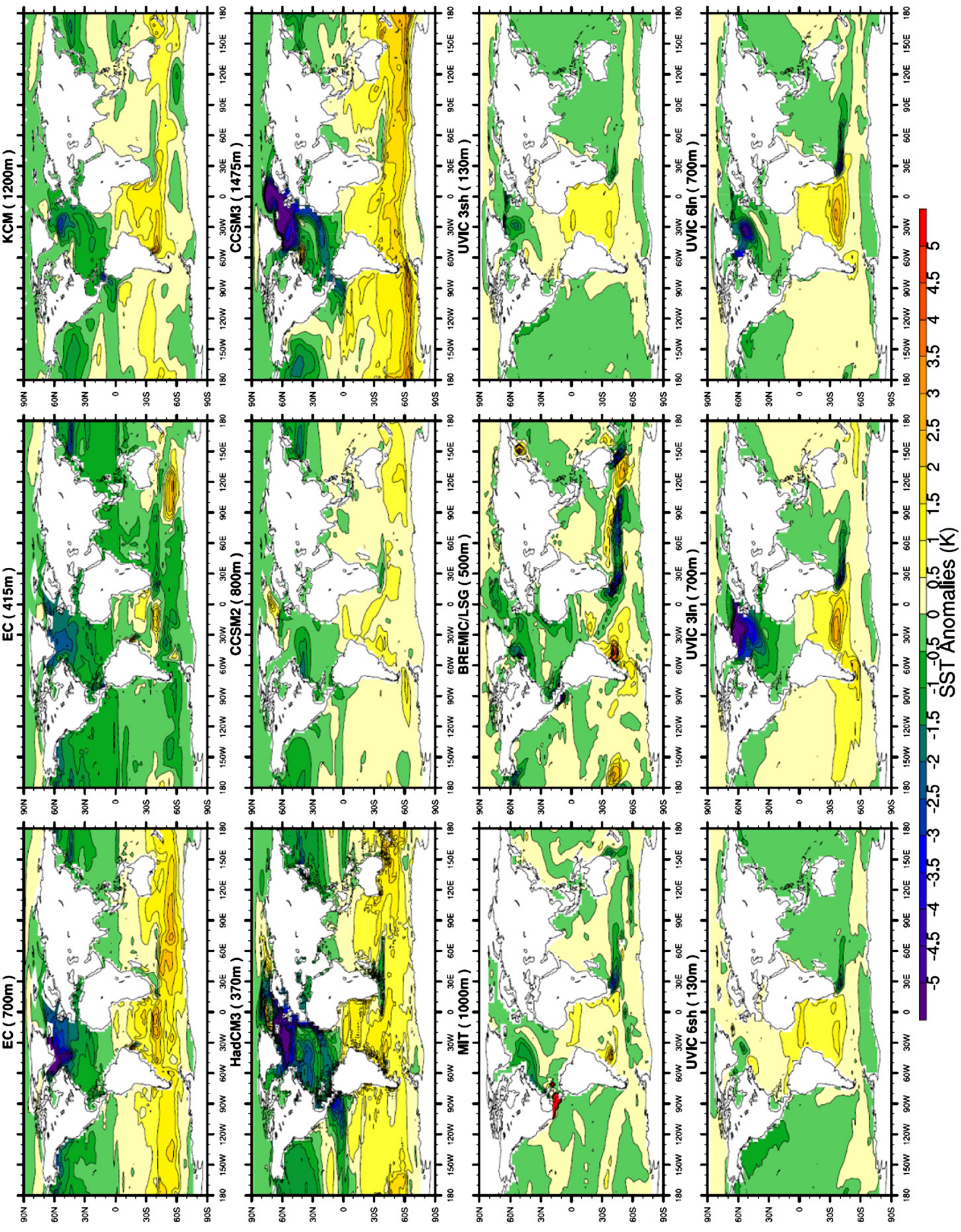
EC ( 700m )
EC ( 415m )
KCM ( 1200m )
HadCM3 ( 370m )
CCSM2 ( 800m )
CCSM3 ( 1475m )
MIT ( 1000m )
BREMIC/LSG ( 500m )
UVIC 3sh ( 130m )
UVIC 6sh ( 130m )
UVIC 3ln ( 700m )
UVIC 6ln ( 700m )
SST Anomalies (K)
-5 -4.5 -4 -3.5 -3 -2.5 -2 -1.5 -1 -0.5 0 0.5 1 1.5 2 2.5 3 3.5 4 4.5 5

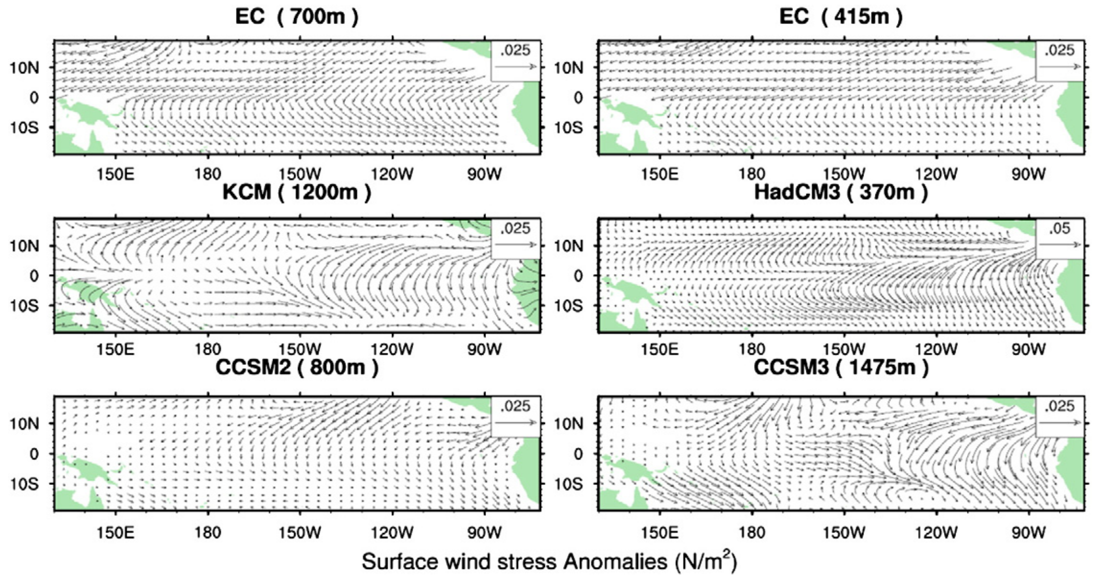


**Fig. 6.** Effect of an open Panamanian seaway on tropical Pacific surface wind stress: Difference in surface wind stress (N/m$^2$) between runs with open and closed Panama gateway (i.e. open minus closed) in the various models that include a dynamic atmosphere. Note the different reference scale of HadCM3 experiment. The depth of the seaway in the different experiments is given in parentheses.

Taken together, the model results strongly support the hypothesis by Steph et al. (2010), which states that intensification of the AMOC – induced by the progressive closure of the Panamanian seaway – played a key role in the Pliocene shoaling of the equatorial Pacific thermocline. This thermocline shoaling was most likely driven by global baroclinic oceanic adjustment and wind-stress changes over the tropical Pacific. It has probably preconditioned the equatorial Pacific cold tongue state, setting the stage for the modern El Niño/ Southern Oscillation (ENSO) system. Proxy records indeed suggest ENSO-related Pacific climate variability after ~3.7 Ma (Scroxton et al., 2011; Von der Heydt and Dijkstra, 2011; Watanabe et al., 2011), while reconstructions for the earlier Pliocene (say, before ~4 Ma) are lacking thus far.

## Acknowledgments

We thank Ralf Tiedemann, Axel Timmermann and Ute Merkel for stimulating discussions. This work has received funding through the DFG Research Center/Excellence Cluster "The Ocean in the Earth System" at the University of Bremen. M.B. is funded through the DFG Research Unit "Understanding Cenozoic Climate Cooling". The CCSM3 climate model experiments were run on the SGI Altix Supercomputer of the "Norddeutscher Verbund für Hoch- und Höchstleistungsrechnen" (HLRN).

## References

Barreiro, M., Philander, G., Pacanowski, R., Fedorov, A.V., 2006. Simulations of warm tropical conditions with application to Middle Pliocene atmospheres. Clim. Dyn. 26, 349–365. doi:10.1007/s00382-005-0086-4.

Broccoli, A.J., Dahl, K.A., Stouffer, R.J., 2006. Response of the ITCZ to Northern Hemisphere cooling. Geophys. Res. Lett. 33, L01702. doi:10.1029/2005GL024546.

Butzin, M., Prange, M., Lohmann, G., 2005. Radiocarbon simulations for the glacial ocean: the effects of wind stress. Southern Ocean sea ice and Heinrich events. Earth Planet. Sci. Lett. 235, 45–61.

Butzin, M., Lohmann, G., Bickert, T., 2011. Miocene ocean circulation inferred from marine carbon cycle modeling combined with benthic isotope records. Paleoceanography 26, PA1203. doi:10.1029/2009PA001901.

Cane, M., Molnar, P., 2001. Closing of the Indonesian seaway as a precursor to east African aridification around 3–4 million years ago. Nature 411, 157–162.

Cannariato, K.G., Ravelo, A.C., 1997. Pliocene–Pleistocene evolution of eastern tropical Pacific surface water circulation and thermocline depth. Paleoceanography 12 (6), 805–820. doi:10.1029/97PA02514.

Cessi, P., Bryan, K., Zhang, R., 2004. Global seiching of thermocline waters between the Atlantic and the Indian–Pacific Ocean Basins. Geophys. Res. Lett. 31, L04302. doi:10.1029/2003GL019091.

Chiang, J.C.H., 2009. The tropics in paleoclimate. Annu. Rev. Earth Planet. Sci. 37, 263–297. doi:10.1146/annurev.earth.031208.100217.

Clement, A.C., Peterson, L.C., 2008. Mechanisms of abrupt climate change of the last glacial period. Rev. Geophys. 46, RG4002. doi:10.1029/2006RG000204.

Collins, D.W., Blackmon, M.L., Bonan, G.B., Hack, J.J., Henderson, T.B., Kiehl, J.T., Large, W.G., McKenna, D.S., 2006. The Community Climate System Model Version 3 (CCSM3). J. Climate 19, 2122–2143.

Dekens, P.S., Ravelo, A.C., McCarthy, M.D., 2007. Warm upwelling regions in the Pliocene warm period. Paleoceanography 22, PA3211. doi:10.1029/2006PA001394.

Fedorov, A.V., Philander, S.G., 2001. A stability analysis of the tropical ocean–atmosphere interactions: bridging measurements of, and theory for El Niño. J. Climate 14, 3086–3101. doi:10.1175/1520-0442(2001) 014.

Fedorov, A.V., Dekens, P.S., McCarthy, M., Ravelo, A.C., deMenocal, P.B., Barreiro, M., Pacanowski, R.C., Philander, S.G., 2006. The Pliocene paradox (mechanisms for a permanent El Niño). Science 312, 1485–1489. doi:10.1126/science.1122666.

Fedorov, A.V., Brierley, C.M., Emanuel, K., 2010. Tropical cyclones and permanent El Niño in the early Pliocene epoch. Nature 463, 1066–1070. doi:10.1038/nature08831.

Goodman, P.J., 2001. Thermohaline adjustment and advection in an OGCM. J. Phys. Oceanogr. 31, 1477–1497. doi:10.1175/1520-0485(2001) 031.

Goosse, H., Fichefet, T., 1999. Importance of the ice–ocean interactions for the global ocean circulation: a model study. J. Geophys. Res. 104 (C10), 23,337–23,355. doi:10.1029/1999JC900215.

Gordon, C., Cooper, C., Senior, C.A., Banks, H., Gregory, J.M., Johns, T.C., Mitchell, J.F.B., Wood, R.A., 2000. The simulation of SST, sea ice extents and ocean heat transports in a version of the Hadley Centre coupled model without flux adjustments. Clim. Dyn. 16, 147–168.

Haarsma, R.J., Campos, E., Hazeleger, W., Severijns, C., 2008. Influence of the meridional overturning circulation on tropical Atlantic climate and variability. J. Climate 21, 1403–1416.

Harrison, D.E., Vecchi, G.A., 2001. El Niño and La Niña: Equatorial Pacific surface temperature and thermocline variability, 1986–98. Geophys. Res. Lett. 28, 1051–1054.

Haywood, A.M., Valdes, P.J., Peck, V.L., 2007. A permanent El Nino-like state during the Pliocene? Paleoceanography 22, PA1213. doi:10.1029/2006PA001323.

Huang, R.X., Cane, M.A., Naik, N., Goodman, P., 2000. Global adjustment of the thermocline in response to deepwater formation. Geophys. Res. Lett. 27 (6), 759–762.

Huybers, P., Molnar, P., 2007. Tropical cooling and the onset of North American glaciation. Clim. Past 3, 549–557.

Jochum, M., Fox-Kemper, B., Molnar, P.H., Shields, C., 2009. Differences in the Indonesian seaway in a coupled climate model and their relevance to Pliocene climate and El Niño. Paleoceanography 24, PA1212. doi:10.1029/2008PA001678.

Kiehl, J.T., Gent, P.R., 2004. The Community Climate System Model, Version 2. J. Climate 17, 3666–3682.

Krebs, U., Park, W., Schneider, B., 2011. Pliocene aridification of Australia caused by tectonically induced weakening of the Indonesian throughflow. Palaeogeogr. Palaeoclimatol. Palaeoecol. 309, 111–117.

Lawrence, K.T., Liu, Z.H., Herbert, T.D., 2006. Evolution of the eastern tropical Pacific through Plio-Pleistocene glaciation. Science 312, 79–83. doi:10.1126/science.1120395.

Lopes dos Santos, R.A., Prange, M., Castañeda, I.S., Schefuß, E., Mulitza, S., Schulz, M., Niedermeyer, E.M., Sinninghe Damsté, J.S., Schouten, S., 2010. Glacial–interglacial variability in Atlantic meridional overturning circulation and thermocline adjustments in the tropical North Atlantic. Earth Planet. Sci. Lett. 300, 407–414.

Lunt, D.J., Valdes, P.J., Haywood, A., Rutt, I.C., 2008a. Closure of the Panama Seaway during the Pliocene: implications for climate and Northern Hemisphere glaciation. Clim. Dyn. 30, 1–18. doi:10.1007/s00382-007-0265-6.

Lunt, D.J., Foster, G.L., Haywood, A.M., Stone, E.J., 2008b. Late Pliocene Greenland glaciation controlled by a decline in atmospheric $CO_2$ levels. Nature 454, 1102–1105.

Maier-Reimer, E., Mikolajewicz, U., Hasselmann, K., 1993. Mean circulation of the Hamburg LSG OGCM and its sensitivity to the thermohaline surface forcing. J. Phys. Oceanogr. 23, 731–757.

Marshall, J., Adcroft, A., Hill, C., Perelman, L., Heisey, C., 1997. A finite-volume, incompressible Navier–Stokes model for studies of the ocean on parallel computers. J. Geophys. Res. 102 (C3), 5753–5766.

McPhaden, M.J., Yu, X., 1999. Equatorial waves and the 1997–98 El Niño. Geophys. Res. Lett. 26 (19), 2961–2964. doi:10.1029/1999GL004901.

Molnar, P., Cane, M.A., 2002. El Niño's tropical climate and teleconnections as a blueprint for pre-Ice-Age climates. Paleoceanography 17 (2). doi:10.1029/2001PA000663.

Nisancioglu, K.H., Raymo, M.E., Stone, P.H., 2003. Reorganization of Miocene deep water circulation in response to the shoaling of the Central American Seaway. Paleoceanography 18 (1), 1006. doi:10.1029/2002PA000767.

Nof, D., Van Gorder, S., 2003. Did an open Panama Isthmus correspond to an invasion of Pacific water into the Atlantic? J. Phys. Oceanogr. 33, 1324–1336. doi:10.1175/1520-0485(2003) 033.

Nof, D., Van Gorder, S., De Boer, A.M., 2007. Does the Atlantic meridional overturning cell really have more than one stable steady state? Deep-Sea Res. I 54 (11), 2005–2021.

Opsteegh, J.D., Haarsma, R.J., Selten, F.M., 1998. ECBilt: a dynamic alternative to mixed boundary conditions in ocean models. Tellus 50A, 348–367.

Park, W., Keenlyside, N., Latif, M., Stroeh, A., Redler, R., Roeckner, E., Madec, G., 2009. Tropical Pacific climate and its response to global warming in the Kiel Climate Model. J. Climate 22, 71–92. doi:10.1175/2008JCLI2261.1.

Prange, M., 2008. The low-resolution CCSM2 revisited: new adjustments and a present-day control run. Ocean Sci. 4, 151–181.

Prange, M., Schulz, M., 2004. A coastal upwelling seesaw in the Atlantic Ocean as a result of the closure of the Central American Seaway. Geophys. Res. Lett. 31, L17207. doi:10.1029/2004GL020073.

Prange, M., Lohmann, G., Paul, A., 2003. Influence of vertical mixing on the thermohaline hysteresis: analyses of an OGCM. J. Phys. Oceanogr. 33 (8), 1707–1721.

Ravelo, A.C., Andreasen, D.H., Lyle, M., Lyle, A.O., Wara, M.W., 2004. Regional climate shifts caused by gradual global cooling in the Pliocene epoch. Nature 429, 263–267. doi:10.1038/nature02567.

Sarnthein, M., Bartoli, G., Prange, M., Schmittner, A., Schneider, B., Weinelt, M., Andersen, N., Garbe-Schönberg, D., 2009. Mid-Pliocene shifts in ocean overturning circulation and the onset of Quaternary-style climates. Clim. Past 5, 269–283.

Schmittner, A., Weaver, A.J., 2001. Dependence of multiple climate states on ocean mixing parameters. Geophys. Res. Lett. 28, 1027–1030.

Schneider, B., Schmittner, A., 2006. Simulating the impact of the Panamanian seaway closure on ocean circulation, marine productivity and nutrient cycling. Earth Planet. Sci. Lett. 246, 367–380. doi:10.1016/j.epsl.2006.04.028.

Scroxton, N., Bonham, S.G., Rickaby, R.E.M., Lawrence, S.H.F., Hermoso, M., Haywood, A.M., 2011. Persistent El Niño-Southern Oscillation variation during the Pliocene epoch. Paleoceanography 26, PA2215.

Steph, S., Tiedemann, R., Prange, M., Groeneveld, J., Nürnberg, D., Reuning, L., Schulz, M., Haug, G., 2006a. Changes in Caribbean surface hydrography during the Pliocene shoaling of the Central American Seaway. Paleoceanography 21, PA4221. doi:10.1029/2004PA001092.

Steph, S., Tiedemann, R., Groeneveld, J., Sturm, A., Nürnberg, D., 2006b. Pliocene changes in tropical East Pacific upper ocean stratification: response to tropical gateways? Proc. Ocean Drill. Program Part B Sci. Results 202, 1–51.

Steph, S., Tiedemann, R., Prange, M., Groeneveld, J., Schulz, M., Timmermann, A., Nürnberg, D., Rühlemann, C., Saukel, C., Haug, G.H., 2010. Early Pliocene increase in thermohaline overturning: a precondition for the development of the modern equatorial Pacific cold tongue. Paleoceanography 25, PA2202. doi:10.1029/2008PA001645.

Stocker, T.F., 1998. The seesaw effect. Science 282, 61–62.

Timmermann, A., An, S.-I., Krebs, U., Goosse, H., 2005. ENSO suppression due to weakening of the North Atlantic thermohaline circulation. J. Climate 18, 3122–3139. doi:10.1175/JCLI3495.1.

Timmermann, A., Okumura, Y., An, S.-I., Clement, A., Dong, B., Guilyardi, E., Hu, A., Jungclaus, J.H., Renold, M., Stocker, T.F., Stouffer, R.J., Sutton, R., Xie, S.-P., Yin, J., 2007. The influence of a weakening of the Atlantic Meridional Overturning Circulation on ENSO. J. Clim. 20, 4899–4919. doi:10.1175/JCLI4283.1.

Tziperman, E., Farrell, B., 2009. Pliocene equatorial temperature: lessons from atmospheric superrotation. Paleoceanography PA1101. doi:10.1029/2008PA001652.

Vecchi, G.A., Soden, B.J., 2007. Global warming and the weakening of the tropical circulation. J. Clim. 20, 4316–4340. doi:10.1175/JCLI4258.1.

Vecchi, G.A., Soden, B.J., Wittenberg, A.T., Held, I.M., Leetmaa, A., Harrison, M.J., 2006. Weakening of tropical Pacific atmospheric circulation due to anthropogenic forcing. Nature 441, 73–76.

Vizcaíno, M., Rupper, S., Chiang, J.C.H., 2010. Permanent El Niño and the onset of Northern Hemisphere glaciations: mechanism and comparison with other hypotheses. Paleoceanography 25, PA2205. doi:10.1029/2009PA001733.

Von der Heydt, A., Dijkstra, H., 2011. El Niño in the Pliocene. Nat. Geosci. 4, 502–503.

Wara, M.W., Ravelo, A.C., Delaney, M.L., 2005. Permanent El Niño-like conditions during the Pliocene warm period. Science 309, 758–761. doi:10.1126/science.1112596.

Watanabe, T., et al., 2011. Permanent El Nino during the Pliocene warm period not supported by coral evidence. Nature 471, 209–211.

Weaver, A.J., et al., 2001. The UVic Earth System Climate Model: model description, climatology and application to past, present and future climates. Atmos. Ocean 39, 361–428.

Yeager, S.G., Shields, C.A., Large, W.G., Hack, J.J., 2006. The low-resolution CCSM3. J. Climate 19, 2545–2566.